

iREVIEWS

STATE-OF-THE-ART PAPERS

Cardiac PET Imaging for the Detection and Monitoring of Coronary Artery Disease and Microvascular Health

Thomas H. Schindler, MD,* Heinrich R. Schelbert, MD, PhD,† Alessandra Quercioli, MD,* Vasken Dilsizian, MD‡

Geneva, Switzerland; Los Angeles, California; and Baltimore, Maryland

Positron emission tomography (PET) myocardial perfusion imaging in concert with tracer-kinetic modeling affords the assessment of regional myocardial blood flow (MBF) of the left ventricle in absolute terms (milliliters per gram per minute). Assessment of MBF both at rest and during various forms of vasomotor stress provides insight into early and subclinical abnormalities in coronary arterial vascular function and/or structure, noninvasively. The noninvasive evaluation and quantification of MBF and myocardial flow reserve (MFR) extend the scope of conventional myocardial perfusion imaging from detection of end-stage, advanced, and flow-limiting, epicardial coronary artery disease (CAD) to early stages of atherosclerosis or microvascular dysfunction. Recent studies have shown that impaired hyperemic MBF or MFR with PET, with or without accompanying CAD, is predictive of increased relative risk of death or progression of heart failure. Quantitative approaches that measure MBF with PET identify multivessel CAD and offer the opportunity to monitor responses to lifestyle and/or risk factor modification and to therapeutic interventions. Whether improvement or normalization of hyperemic MBF and/or the MFR will translate to improvement in long-term cardiovascular outcome remains clinically untested. In the meantime, absolute measures of MBF with PET can be used as a surrogate marker for coronary vascular health, and to monitor therapeutic interventions. Although the assessment of myocardial perfusion with PET has become an indispensable tool in cardiac research, it remains underutilized in clinical practice. Individualized, image-guided cardiovascular therapy may likely change this paradigm in the near future. (J Am Coll Cardiol Img 2010;3: 623–40) © 2010 by the American College of Cardiology Foundation

From the *Nuclear Cardiology and Cardiac Imaging, Division of Cardiology, Department of Medicine, University Hospitals of Geneva, Geneva, Switzerland; †Department of Molecular and Medical Pharmacology, David Geffen School of Medicine at UCLA, Los Angeles, California; ‡Department of Radiology and Nuclear Medicine, University of Maryland School of Medicine, Baltimore, Maryland. Dr. Schindler is supported by grants from the Swiss National Science Foundation (SNF grant: 3200B0-122237), and the Department of Internal Medicine of the University Hospitals of Geneva; Dr. Quercioli is supported by Fellowship grants from the Novartis Research Foundation; and Professor Schelbert is supported by Research Grant HL 33177, from the National Heart, Lung and Blood Institute.

Manuscript received February 11, 2010; revised manuscript received April 21, 2010, accepted April 26, 2010.

Despite aggressive medical and interventional therapies, morbidity and mortality that is attributable to coronary artery disease (CAD) remains high (1). There is a striking increase in the prevalence of obesity and type 2 diabetes mellitus in the U.S., which poses a considerable public health concern (2). In particular, patients with type 2 diabetes mellitus exhibit accelerated progression of CAD, which may account for the increased morbidity and mortality in these patients (2). Another area of a cardiovascular health concern is the expected increase in the longevity of post-menopausal women. Unlike pre-menopausal women who benefit from endogenous atheroprotective estrogens, the cardiovascular risk profile in post-menopausal women becomes comparable to that of age-matched men, exhibiting higher total cholesterol, low-density lipoprotein cholesterol, triglycerides, and lower high-density lipoprotein levels as well as increases in body weight and arterial hypertension, all known to be proatherogenic (3). According to the Framingham Heart Study (4), individuals with a high cardiovascular risk profile, such as type 2 diabetes mellitus or multiple coronary risk factors, are at risk for future cardiovascular events, and are commonly referred for primary and secondary medical prevention of CAD (5–7). Individuals with an intermediate cardiovascular risk, however, may not necessarily be considered for preventive medical interventions and/or life style modifications.

Apart from standard myocardial perfusion imaging, noninvasive assessment of absolute myocardial blood flow (MBF) with positron emission tomography (PET), in milliliters per gram per minute (ml/g/min), opens opportunities for a comprehensive evaluation of asymptomatic and/or early stages of symptomatic CAD. Assessment of coronary vascular function with PET may further risk stratify individuals with an intermediate cardiovascular risk (8–10). For example, impaired MBF responses to vasomotor stress have been shown to independently predict the development of CAD (11–14). Other possible surrogate markers for sub-clinical CAD include measurements in carotid intima-media thickness determined by vascular ultrasound (15), or coronary artery calcification and/or coronary morphology by multidetector computed tomography (CT) (16,17). Assessment of functional abnormalities of the coronary vessels with PET may have an advantage over structural

alterations of the arterial wall, as it may identify the earliest functional stage of the initiation and development of the coronary atherosclerotic process before structural alterations within the arterial wall may manifest (18). If CAD-related functional abnormalities of the coronary circulation precede morphologic changes of the vessels (8,9,19,20), then PET could emerge as a promising tool to better identify asymptomatic individuals with an intermediate or even low cardiovascular risk, who are likely to benefit from an early initiation or intensified medical preventive therapy (8,21).

Methodological Considerations of PET Flow Quantification

PET approaches for the assessment of regional MBF in ml/g/min entails the intravenous injection of a positron-emitting perfusion tracer, such as ^{13}N -ammonia, ^{15}O -water, or ^{82}Rb idium, and dynamic acquisition of images of the radiotracer passing through the central circulatory system to its extraction and retention in the left ventricular myocardium (Table 1) (19,22,23). Tracer-kinetic models (1 to 3 compartments) and operational equations are then applied to correct for physical decay of the radioisotope, partial volume-related underestimation of the true myocardial tissue concentrations (by assuming a uniform myocardial wall thickness of 1 cm) (24), and spillover of radioactivity between the left ventricular blood pool and myocardium (25), to yield regional MBFs in absolute terms, ml/g/min (Figs. 1 and 2) (19,26). The relative distribution of the radiotracer in the myocardium can also be assessed visually or semiquantitatively (as percentage uptake relative to a reference region) from the final static image of the myocardium, obtained from the last (e.g., 900 s) frame of the PET image series (27).

PET Myocardial Perfusion Tracers

The quantification of MBF in absolute units has been validated for ^{13}N -ammonia and ^{15}O -water against independent microsphere blood flow measurements in animals over a flow range of 0.5 to 5.0 ml/g/min (28–32). In human subjects, ^{13}N -ammonia and ^{15}O -water provide similar absolute MBF information over a wide range of blood flows (33,34). However, ^{15}O -water images of the myocardium are usually of lower count density, due to its short physical and biological half-life in the myocardium (Table 1), thereby limiting the visual

ABBREVIATIONS AND ACRONYMS

CAD = coronary artery disease
CPT = cold pressor test(ing)
CT = computed tomography
MBF = myocardial blood flow
MFR = myocardial flow reserve
PET = positron emission tomography
SPECT = single-photon emission computed tomography

Table 1. Radiotracers Characteristics and Image Acquisition for PET Perfusion Imaging and MBF Quantification

Characteristics	⁸² Rubidium	¹³ N-Ammonia	¹⁵ O-Water
Half-life	78 s	9.8 min	2.4 min
Extraction fraction*	≈60%	≈80%	≈95%
Cyclotron on-site	No	Yes	Yes
Data acquisition	Dynamic, static, gated	Dynamic, static, gated	Dynamic
Scan duration	6 min	20 min	5 min
Dose—2D	40–60 mCi	15–25 mCi	40 mCi
Dose—3D	15–20 mCi 30–40 mCi 3D LSO	15 mCi	10 mCi
Interval between doses	10 min	30 min	7 min
Image interpretation	Yes	Yes	No
Image quality	Good	Excellent	N/A

*Extraction fractions are listed for baseline MBF (≈1 ml/g/min).
2D = 2-dimensional; 3D = 3-dimensional; LSO = lutetium oxyorthosilicate; MBF = myocardial blood flow; N/A = not applicable; PET = positron emission tomography.

or semiquantitative assessment of regional myocardial perfusion from the static images. Unlike ¹⁵O-water static images of the myocardium, ¹³N-ammonia yields high-contrast resolution myocardial perfusion images (8,26). The latter is due to the combination of the high first-pass myocardial extraction fraction of ¹³N-ammonia (near 80%), trapping of ¹³N-ammonia in the myocardial cells as ¹³N-glutamine (long biological half-life), and the relatively long physical half-life (9.8 min) of the ¹³N radiotracer. These properties of ¹³N-ammonia per-

mit the acquisition of statistically high count images of the myocardium by PET with a high diagnostic quality for the visual and semiquantitative assessment of myocardial perfusion defects during stress and rest (Fig. 3) (35). The concurrent evaluation of regional MBFs at rest and during various forms of vasomotor stress with ¹³N-ammonia PET and tracer-kinetic models enables the identification and characterization of subclinical and early stages of the coronary atherosclerotic process (8,19,36–38).

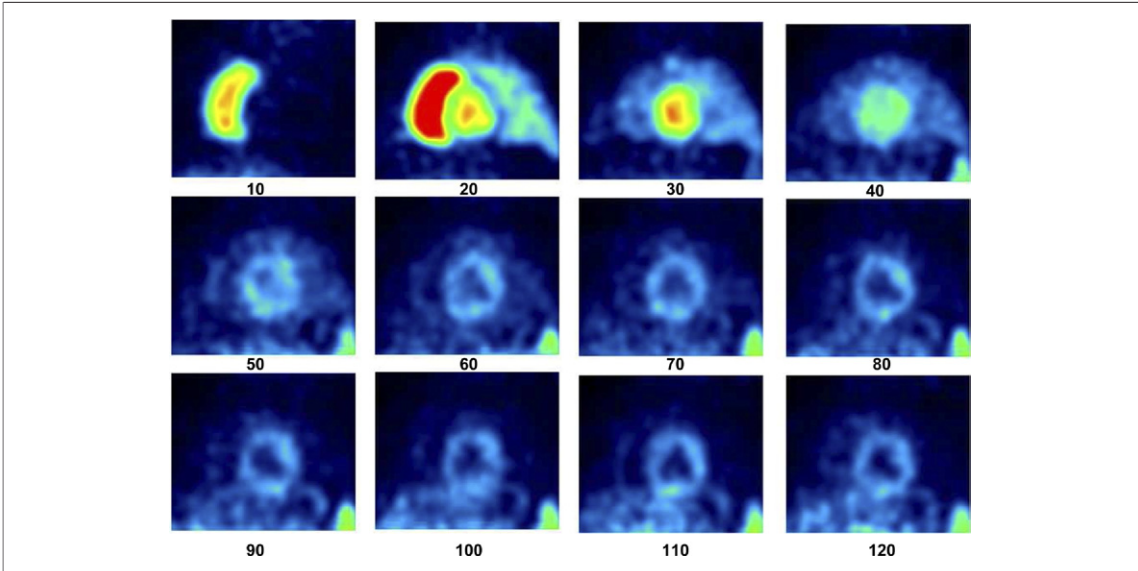
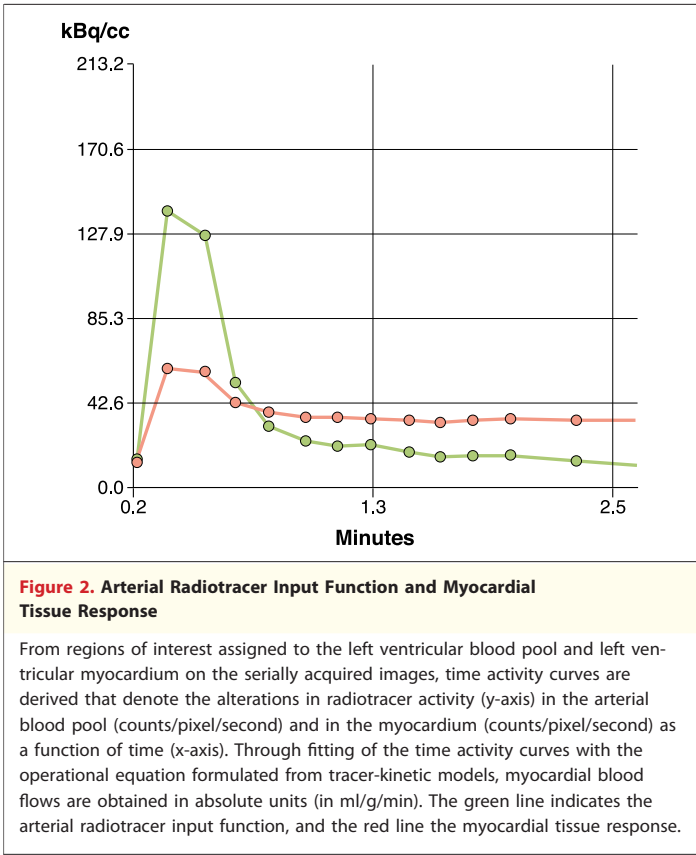


Figure 1. Serially Acquired Images of a Bolus Transit of ¹³N-Ammonia Through the Central Circulation

The serially acquired 10-s short-axis images denote the transit of the intravenously applied radiotracer bolus through the central circulation (from left to right and top to bottom). The initial 2 images illustrate the tracer activity mostly in the right ventricular cavity. Subsequently, the tracer bolus is dispersed into both lungs and returns into the left ventricular cavity, as shown in image 3. This is followed by a clearance of the tracer activity from the arterial blood pool into the myocardium (serial 10-s images). The late static image after 18 min (not shown), displays the tracer activity retained in the left ventricular myocardium after the radiotracer has widely disappeared from the blood pool.



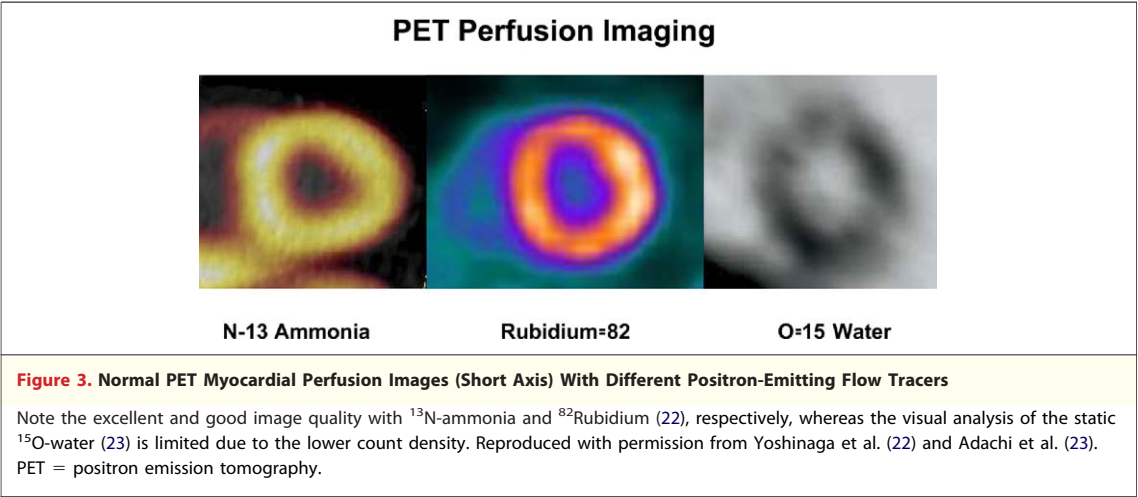
In the clinical setting, ^{13}N -ammonia and ^{82}Rb -rubidium are the only PET myocardial perfusion tracers that have received U.S. Food and Drug Administration approval. ^{82}Rb -rubidium for PET myocardial perfusion imaging is increasingly used in the clinical routine as it affords the advantages of an ultra-short 75-s physical half-life and its independency of an onsite cyclotron through the availability of a Strontium-82/Rubidium-82 generator system

with a 4- to 5-week shelf life. However, its relatively lower first-pass extraction and the more prominent nonlinear myocardial uptake with increasing blood flow, termed “roll-off phenomenon,” may lead to relatively lower myocardial contrast resolution images when compared with ^{13}N -ammonia (Fig. 3). Despite the known limitations of flow-dependent extraction fraction of ^{82}Rb -rubidium for quantification of MBF, recent clinical investigations have reported promising results (39–41).

More recently, F-18-labeled perfusion tracer was introduced for myocardial perfusion imaging with PET (42,43). The radiotracer has a high first-pass extraction fraction of 94%, and is currently being evaluated in phase 1 and 2 clinical studies. The 110-min half-life of F-18 permits its distribution as a single-unit dose on a daily basis. Moreover, the longer half-life of F-18 allows the application of the perfusion agent during treadmill exercise, rather than with vasodilator stress alone, as is currently the case with ^{82}Rb -rubidium PET myocardial perfusion studies.

Clinical Utility of Quantification of Myocardial Blood Flow with PET

Assessment of stress-induced myocardial perfusion defects, with single-photon emission tomography (SPECT) or PET, have been firmly established as an important diagnostic and prognostic tool for the evaluation of patients with suspected CAD (44,45). However, there are distinct limitations with visual or semiquantitative assessment of regional myocardial perfusion defects that may be overcome by absolute quantification with PET. The noninvasive evaluation and quantification of MBF and myocardial flow reserve (MFR) extends the scope of



conventional myocardial perfusion imaging from detection of end-stage, advanced and flow-limiting, epicardial CAD to early stages of atherosclerosis or microvascular dysfunction, as in: 1) the identification of subclinical CAD; 2) the improved characterization of the extent and severity of CAD burden; and 3) the identification of “balanced” reduction of MBF in all vascular territories.

Identification of subclinical CAD. In symptomatic patients with known or suspected CAD, SPECT myocardial perfusion imaging is accurate for identifying flow-limiting epicardial coronary lesions (46,47). However, vascular disease at the microcirculatory level of the coronary circulation or early stages of subclinical CAD may remain undetected with the standard myocardial perfusion SPECT imaging (32). Patients with subclinical stages of CAD may exhibit either subtle heterogeneity in relative myocardial uptake of the radiotracer or homogeneously impaired hyperemic blood flow of the left ventricular myocardium. These same individuals with early stages of CAD-related functional and/or structural alterations of the coronary arterial wall have been shown to be at increased long-term risk for cardiovascular events (12,13). By quantifying hyperemic MBF or MFR in absolute terms, PET can identify early functional abnormalities of the coronary circulation, which may be a precursor of the ensuing CAD process (8,13,48–50).

Improved characterization of CAD burden. Decreased regional radiotracer uptake on standard SPECT or PET myocardial perfusion imaging during hyperemic flow are a consequence of flow-limiting epicardial coronary artery lesions. Visual or semiquantitative interpretation of regional radiotracer uptake is in relative terms, where the myocardial region with the highest radiotracer uptake is considered as the “normal reference region.” However, in patients with multivessel CAD, the designated normal reference region may in fact be abnormal as well, but relative to the other vascular territories it is the least hypoperfused myocardial region (51–53). In such patients, the concurrent absolute MBF or MFR assessment with PET may uncover, not only the most hemodynamically significant culprit lesion, but also the true extent of ischemic burden in the left ventricular myocardium, in a multivessel territory, which includes the normal reference region (53,54). Thus, the combined assessment of “relative” and “absolute” myocardial perfusion imaging provides information,

not only on flow-limiting isolated epicardial lesions, but also on the downstream functional consequences of anatomically intermediate and/or sequential coronary artery lesions, or continuous tapering of coronary artery vessel due to diffuse atherosclerosis (55–57).

Identification of “balanced” reduction of MBF in all vascular territories. The assessment of only “relative” distribution of the radiotracer uptake in the left ventricular myocardium with standard myocardial perfusion imaging may also fail to identify “balanced” reduction of MBF in all vascular territories. In such patients, the relative distribution of myocardial perfusion may be homogeneously reduced in the entire left ventricular myocardium without visually discernable regional defects that characterize CAD patients (52). Consequently, only about 10% of patients with severe 3-vessel CAD or significant stenosis of the left main coronary artery ($\geq 50\%$) may be detected by stress-induced regional perfusion defects on SPECT images (51,58). The addition of gated SPECT functional data may improve the identification of patients with severe 3-vessel CAD or left main disease to 25% (59). A more direct assessment of absolute MBF of MFR with PET may unmask balanced ischemic burden of the left ventricular myocardium in all 3 major coronary artery vascular territories. The latter, however, should always be confirmed by a peak stress transient ischemic cavity dilation of the left ventricle during maximal vasomotor stress on gated PET images (60,61).

Evaluation of Flow-Limiting Epicardial Lesions: Advantages of PET

The high spatial and contrast resolution of the photon attenuation-free images of PET in concert with superior properties of ^{13}N -ammonia or ^{82}Rb -rubidium as MBF tracers offers several advantages of PET over SPECT for detection of CAD. PET cameras identify paired photons (511 keV of energy each) produced by the positron annihilation effect (Fig. 4). The paired 511 keV travel in the opposite direction at a 180° angle from each other. Therefore, positron decay can be localized without collimation, as used for SPECT, but with the use of the principle of coincidence detection. As PET cameras do not necessitate collimators, these systems have a much higher sensitivity than do SPECT cameras, resulting in a higher spatial resolution in the range of 4 to 7 mm (62). The principle of coincidence detection in concert with the superior properties of

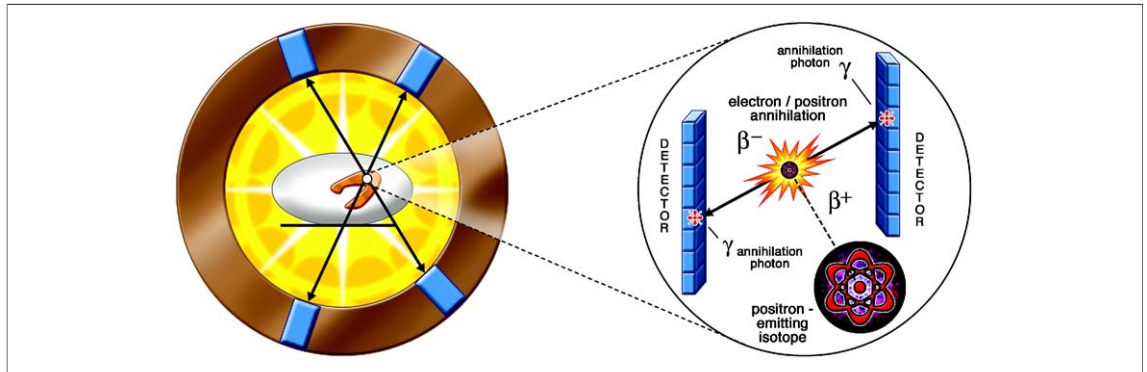


Figure 4. Principles of Coincidence Detection

A positron (β^+) emitted from the atomic nucleus of ^{13}N travels through a medium and loses energy and slows down until it interacts with an electron (e^-). Since the e^- and β^+ are antiparticles, they undergo a process called “annihilation.” The latter manifests in the generation of 2 photons traveling in opposite directions at a 180° angle from each other with an energy of 511 keV each. These photons are identified as coincidences in the detector ring of the PET camera. PET = positron emission tomography.

MBF tracers such as ^{13}N -ammonia with a better extraction fraction at higher flows has also led to an increase in contrast resolution (Table 1) (Fig. 3). Both the higher spatial and contrast resolution of PET perfusion studies may allow the identification of regional differences in radiotracer uptake during pharmacologically induced hyperemia (Fig. 5). These properties of PET perfusion imaging may explain, at least in part, the higher sensitivity in the identification of flow-limiting epicardial lesions as compared with SPECT imaging with ^{201}Tl or $^{99\text{m}}\text{Tc}$ -labeled perfusion tracers (19). The average sensitivity and specificity of myocardial perfusion PET or PET/CT scanners for detecting $\geq 50\%$ or $\geq 70\%$ luminal narrowing on coronary angiography is reported to be in the mean of 92% and 90%, respectively (63–65). The increase in specificity of PET perfusion imaging as compared with SPECT (66,67) can be related to the robust attenuation correction of the emission data using the transmission source (^{68}Ge rotating rod source or CT) (Fig. 6).

Concordance and Discordance Between Coronary Artery Narrowing and Myocardial Perfusion Abnormality

Quantitative coronary angiography (QCA) is commonly accepted as a “gold standard” for the assessment of the epicardial coronary artery diameter and luminal narrowing (68). When epicardial luminal narrowing exceeds 50%, it is commonly paralleled by a decrease in MBF reserve and manifestation of myocardial ischemia (69–72). It should be kept in mind, however, that despite the well-described

inverse relationship between severity of coronary artery stenosis and MFR, a high degree of variability in the individual flow responses may exist, in particular when the coronary artery luminal narrowing is of intermediate severity (Fig. 7) (56,69,71). In the case of CT-determined luminal narrowing, stress-induced regional myocardial perfusion defects as determined with ^{201}Tl SPECT were seen in 33% of regions with 60% to 70% stenosis, 54% of regions with 70% to 80% stenosis, and 86% of regions with $\geq 80\%$ stenosis (73). Beyond an adaptive vasodilation of the coronary arteriolar vessels to compensate increases in epicardial resistance due to significant epicardial narrowing of the arterial lumen (56,57), other possible explanations for the discordances in the literature include an overestimation of the severity of coronary artery stenosis by angiography and/or a lack of absolute regional MBF assessment with the perfusion data. Nonetheless, a relatively preserved regional hyperemic MBF or MFR may in fact prevent the manifestation of stress-induced myocardial ischemia even in the presence of intermediate to severe epicardial artery lesions. Thus, medical therapy that targets and improves the function of the coronary artery circulation or its vasodilator capacity, e.g., HMG-CoA reductase or angiotensin-converting enzyme inhibitors, may prevent or even regress clinically manifest myocardial ischemia in patients with CAD (74,75). This possibility is supported by the recent subanalysis of the COURAGE (Clinical Outcomes Utilizing Revascularization and Aggressive Drug Evaluation) trial (45). Medical treatment of cardiovascular risk factors in patients with SPECT-determined regional myocardial perfusion defects

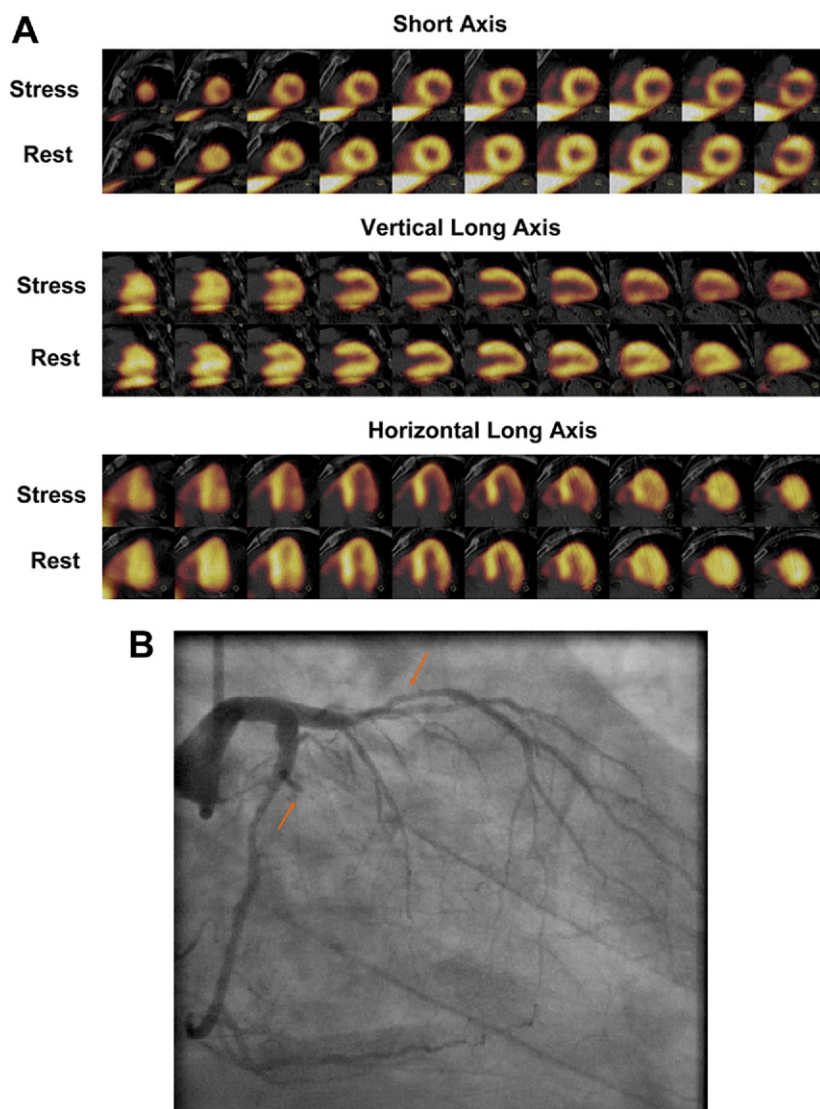


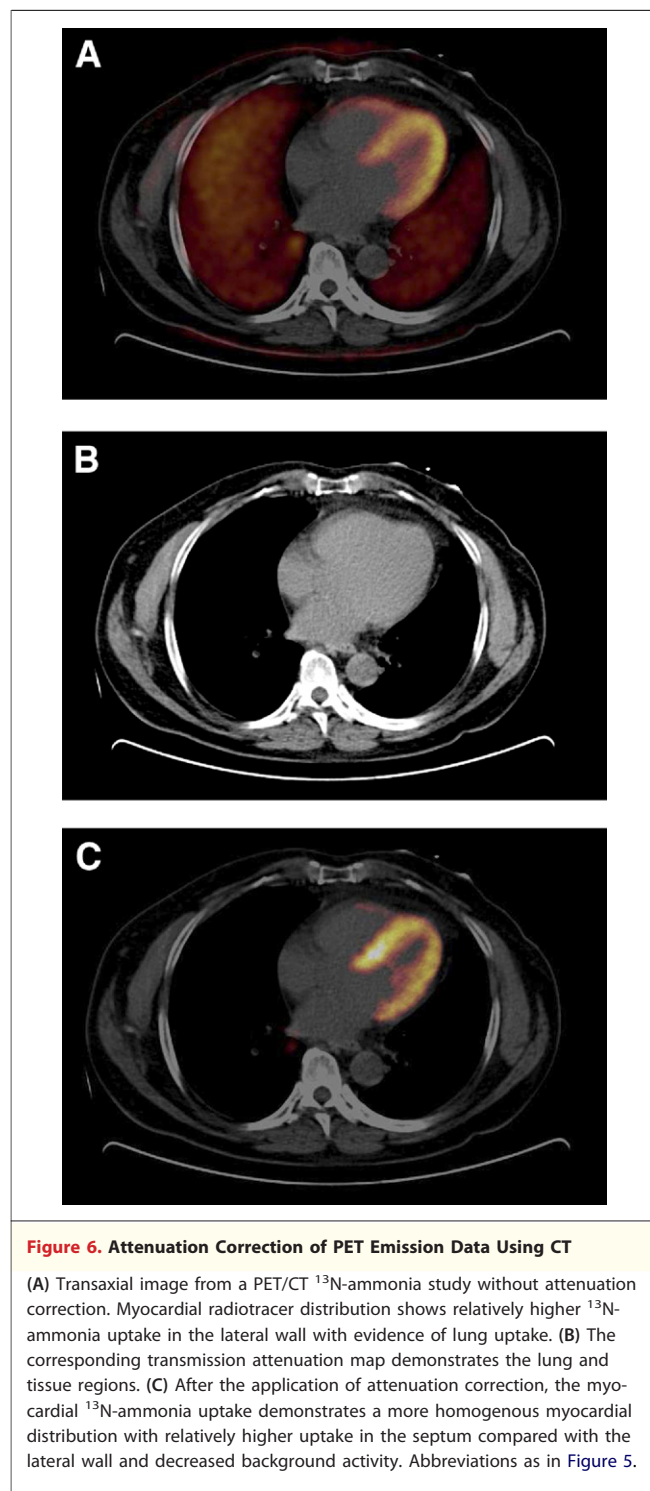
Figure 5. ^{13}N -Ammonia PET/CT and Coronary Angiography in the Evaluation of CAD

(A) Stress and rest ^{13}N -ammonia PET images of the heart in short-axis, vertical long-axis, and horizontal long-axis slices are shown from a 62-year-old type 2 diabetic patient. The stress images demonstrate a moderately decreased perfusion defect involving the lateral extending to the inferolateral region of the left ventricle, which is completely reversible on rest images. (B) Corresponding coronary angiography shows an occluded marginal branch of the left circumflex coronary artery (arrow), with diffuse 50% stenosis of the proximal left anterior descending coronary artery (arrow) and a 50% stenosis in the mid right coronary artery (not shown). CAD = coronary artery disease; CT = computed tomography; PET = positron emission tomography.

over a 1-year follow-up targeting the improvement of MBF reserve was associated with a significant reduction in ischemic burden and a favorable clinical outcome. Another factor that is likely to prevent the manifestation of stress-induced regional ischemia is the induction of collaterals by the hypoxic stimulus, which strive to balance reduced flow increases during times of increased metabolic demand in myocardial regions subtended by flow-limiting epicardial lesions (76).

Assessment of Hyperemic MBF, MFR, and Relative Radiotracer Content

The ability of PET to assess regional MBF at rest and during vasomotor stress, concurrently, affords absolute quantification of regional hyperemic MBFs and MFR, by which, apart from the “culprit lesion” causing the stress-induced regional myocardial perfusion defect, the hemodynamic significance of each epicardial lesion can be identified in all 3



vascular territories. The optimal threshold values of hyperemic MBFs or MFR to identify flow-limiting epicardial lesions, however, is dependent on the PET methodology and radiotracer applied for the MBF quantification (19,36,56). Among patients with known or suspected CAD undergoing phar-

macologic vasodilation with ^{13}N -ammonia PET, the diagnostic value of hyperemic MBF, MFR, and the relative radiotracer content (millicuries per milliliter) for detecting $\geq 70\%$ flow-limiting epicardial lesions was the highest, when a hyperemic MBF threshold value of < 1.85 ml/g/min was applied (67). The receiver-operator characteristic analysis of PET parameters in the evaluation of the diagnostic accuracy of CAD demonstrated the highest value of 0.90 for adenosine-stimulated absolute hyperemic MBF, 0.86 for MFR, and 0.69 for ^{13}N -ammonia relative uptake (77,78). Similar findings were recently reported by other investigators (79,80). Using ^{15}O -water, a threshold of pharmacologically induced hyperemic MBFs of 2.5 ml/g/min was shown to be most accurate in the identification of epicardial lesions of $> 50\%$ diameter stenosis (79). Another investigation using quantitative ^{82}Rb -rubidium PET demonstrated a nonlinear decrease in hyperemic MBFs as the severity of coronary artery stenosis increased (80). It appeared that the MFR could differentiate epicardial lesions between 70% to 80% from those with 50% to 69% stenosis.

Hyperemic MBFs during pharmacologic vasodilation may also be diminished due to coronary microvascular dysfunction in patients with or without focal CAD lesions on coronary angiography but with multiple cardiovascular risk factors (49,81,82). Furthermore, a grey zone may exist in patients with epicardial lesions $\geq 50\%$ and a MBF reserve between 2.0 and 2.5, where the significance of downstream consequences of a focal epicardial lesion may remain uncertain. Overall, adding PET-determined regional hyperemic MBFs and MFR to standard myocardial perfusion imaging certainly increases the sensitivity in the identification of each flow-limiting epicardial lesion in multivessel disease but at the expensive of a lower specificity (83,84). Whether this approach may play a role in the future for revascularization planning with percutaneous interventions or coronary artery bypass surgery, or both (so-called hybrid interventions) in patients with multivessel CAD remains uncertain and requires clinical validation. Current clinical application of myocardial perfusion imaging with PET is aimed at differentiating normal vasomotor stress response from hemodynamically significant coronary artery lesions (stress-induced regional perfusion defect) (Fig. 8) and subclinical CAD (Fig. 9). Among individuals with high cardiovascular risk who exhibit reduced hyperemic MBF and MFR on PET but without significant epicardial coronary artery luminal narrowing, preventive medical inter-

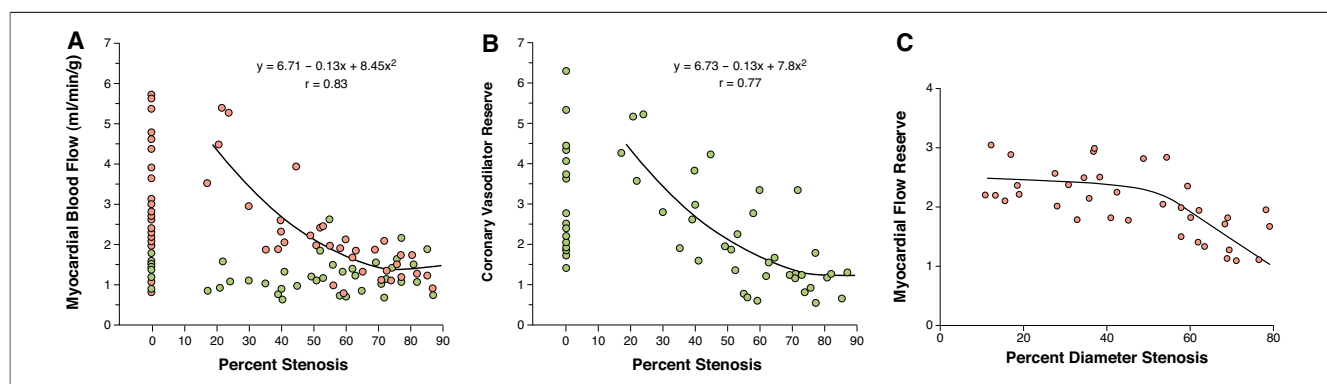


Figure 7. MBF and Coronary Vasodilator Reserve in Relation to Percentage Coronary Artery Diameter Stenosis

(A) At rest (green circles), there is no relationship between myocardial blood flow (MBF) and percentage coronary artery stenosis. During pharmacologic vasodilation (red circles), there is an inverse relationship between hyperemic MBFs and percentage coronary artery stenosis. (B) Similar to hyperemic MBFs, myocardial (or coronary) flow reserve (MFR = hyperemic MBF / resting MBF) shows a similar inverse relationship with percentage coronary artery stenosis (69). However, for coronary stenoses of intermediate severity, there was a relatively high variability in MFR. Notably, in individuals without epicardial coronary artery stenoses, reductions in hyperemic MBFs or the MFR due to microvascular disease may be comparable to those in myocardial regions subtended by epicardial lesions $\geq 50\%$ diameter stenosis. (C) The observed relationship between MFR and percentage stenosis persists when the severity of coronary artery lesions are determined with quantitative coronary angiography (correlation coefficient $r = 0.77$, root mean square error = 0.37, $p < 0.00001$) (71). Panels A and B are reproduced with permission from Uren et al. (69); panel C is reproduced from Di Carli et al. (71).

vention and lifestyle modifications may apply. However, in view of the relatively low specificity of abnormal MBF reserve (69,85), current application and interpretation of MBF reserve with PET have to be placed in the proper clinical context with underlying coronary anatomy and cardiovascular risk factors (Fig. 9).

Assessment of Subclinical Stages of CAD and Prognosis

In patients exhibiting normal SPECT or PET myocardial perfusion studies by relative radiotracer content, the assessment of impaired hyperemic MBFs and MFR by absolute quantitative PET (49,81,86) may further identify individuals who are at increased risk for cardiovascular events (12,13,87). For example, in insulin-resistant individuals with normal stress-rest myocardial perfusion PET images, concurrent MBF quantification has uncovered abnormalities in endothelium-related MBF responses to cold pressor testing (CPT), whereas hyperemic flows during pharmacologic vasodilation were preserved (88). These observations support the contention that initial stages of the vascular injury may involve only the endothelium (89–91), whereas more advanced stages of coronary risk factor states, such as increases in oxidative stress burden, may lead to an impairment in smooth muscle cell vasodilator function (92). Indeed, coronary circulatory dysfunction in individuals with increasing body weight may progress from an im-

pairment in endothelium-dependent coronary flow response to CPT, in the early stages of overweight, to an impairment of the predominantly endothelium-independent hyperemic flows during dipyridamole stimulation in the late stages of obesity (49). Similarly, in patients with insulin resistance, progressive worsening of functional abnormalities of endothelium-dependent vasomotion may occur with increasing severity of insulin resistance and carbohydrate intolerance, with attenuation of the total vasodilator capacity occurring in the later stages, in patients with clinical type 2 diabetes mellitus (70). An inverse relationship between MFR and plasma glucose levels has been shown in patients with type 2 diabetes mellitus, providing first evidence of direct adverse effect of raised plasma glucose concentration on diabetes-related coronary vasculopathy (88).

In individuals with increased cardiovascular risk, the assessment of MBF response to CPT may provide the earliest insight into coronary endothelial (dys)function as a precursor to progression of CAD and its prognostic consequence (8,18,50). In patients with normal coronary angiograms, but with cardiovascular risk factors, attenuation of PET-measured and endothelium-related MBF responses to sympathetic stimulation with CPT and its MFR were associated with a higher risk for cardiac events as compared with those with normal flow increases (12). Moreover, the incidence of cardiovascular events increased with the extent of abnormal flow response to CPT (Fig. 10). Others have shown that

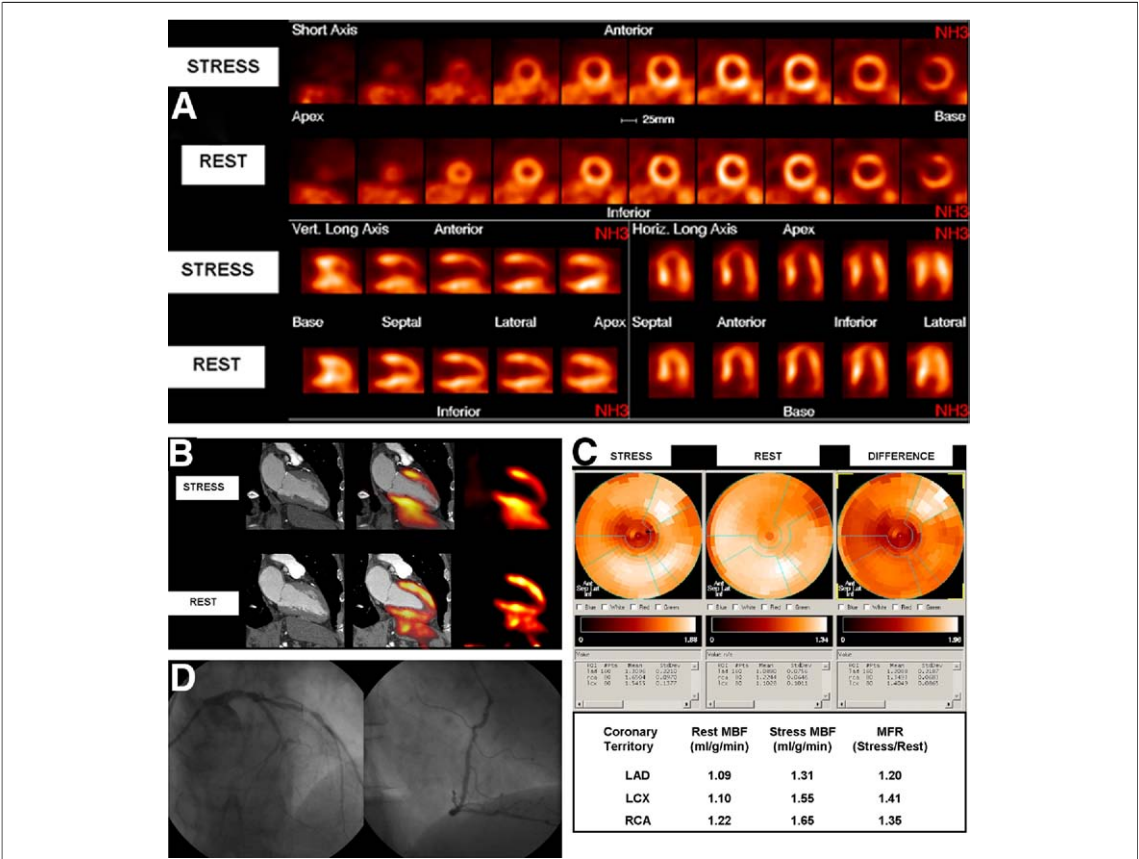


Figure 8. ¹³N-Ammonia PET in the Evaluation of CAD

(A) Myocardial perfusion study with ¹³N-ammonia PET during dipyridamole stimulation and at rest in a 61-year-old patient with arterial hypertension and type 2 diabetes mellitus. On stress images, there is a moderately decreased perfusion defect involving the mid-to-distal anterior, anteroseptal, and apical regions of the left ventricle, which becomes reversible on the rest images. Uptake is preserved in the lateral and inferior regions. (B) Stress and rest integrated PET/CT images of the left ventricular myocardium are shown (middle panel). Integrated PET/CT image allows an accurate coregistration of relatively low spatial resolution of the ¹³N-ammonia perfusion signal of PET with the high-resolution anatomic signal of the CT-contrast image. For direct comparison, ¹³N-ammonia PET perfusion images (right panel) and CT-contrast images with delineation of the left ventricular cavity and myocardial wall (left panel) are shown prior to integration. (C) Polar maps of ¹³N-ammonia PET during dipyridamole stimulation, at rest, and the difference between stress and rest are displayed in terms of absolute regional myocardial blood flow (MBF) (upper panel) and within the 3 major vascular territories (lower panel) are shown (Munich Heart Program software package, S. Nekolla). The summarized quantitative data (lower panel), suggests a distinct impairment of the MFR not only in the left anterior descending artery (LAD) territory, but also in the right coronary artery (RCA), and left circumflex artery (LCX) vascular territories (MFR <2.0). (D) Coronary angiography in this patient demonstrated a proximal occlusion of the LAD, 80% stenosis in the proximal segments of the LCX (left panel), and sequential 50% to 60% lesions in the RCA (right panel) (53). Abbreviations as in Figures 3 and 5.

beyond reduced MFR, stress-induced myocardial perfusion defects is also an independent predictor of cardiovascular outcome (9). However, adding the MFR information to the stress ¹³N-ammonia perfusion PET data allowed further risk stratification, identifying a “warranty” period of event-free survival of 3 years when both stress myocardial perfusion and MFR data were normal. Contrarily, when both stress myocardial perfusion and MFR data were abnormal, impaired MFR provided incremental information to the stress ¹³N-ammonia perfusion PET data for predicting adverse outcomes. It is important to highlight the prognostic differences

between stress myocardial perfusion SPECT or PET studies and PET-assessment of coronary circulatory dysfunction. Whereas the presence of stress-induced myocardial perfusion defects on SPECT or PET is predictive of cardiovascular events during a shorter follow-up period of time (e.g., 1 year), PET assessment of coronary circulatory dysfunction in patients without flow-limiting epicardial coronary artery lesions commonly predicted future cardiovascular events (e.g., after 2 to 3 years) (12,13,27,87,93,94). Consequently, the assessment of coronary circulatory dysfunction with PET may identify individuals with cardiac risk

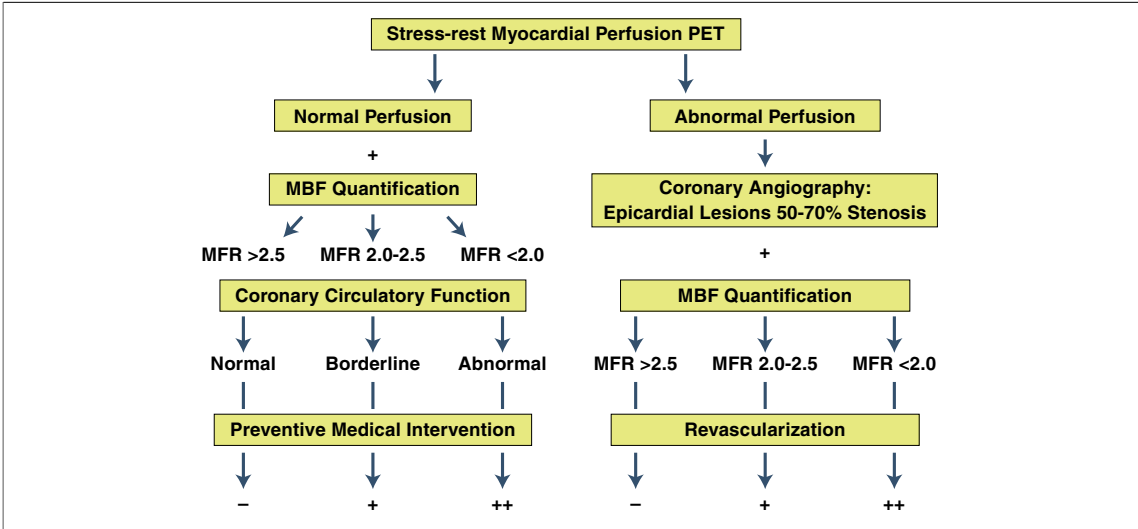


Figure 9. Algorithm for the Integration of PET Perfusion Images and MFR
Algorithm for the integration of PET myocardial perfusion imaging and absolute myocardial blood flow (MBF) and flow reserve (MFR) quantification in individuals with suspected or an intermediate risk for developing CAD for clinical decision making towards revascularization or preventive medical therapy is shown. Abbreviations as in Figures 3 and 5.

factors, who are at risk of developing CAD and its atherothrombotic sequelae.

Beyond its incremental value in individuals with CAD or subclinical stages of CAD, impairment in coronary circulatory function has also been shown to be predictive of future cardiovascular outcome in patients without underlying CAD, such as those with hypertrophic cardiomyopathy and idiopathic cardiomyopathy (10,95). Such clinical observations emphasize the importance of integrating coronary circulatory function as an index of the overall stress burden imposed by various coronary risk factors on the arterial wall (8,96).

Reproducibility of MBFs During Vasomotor Stress

If impaired coronary circulatory function is a predictor of future cardiovascular events, then medical interventions or lifestyle modifications, that improve or normalize the coronary circulatory function, would be expected to improve patient outcome. In view of this evolving concept, PET measurements of MBF responses to cold exposure and/or to pharmacologic vasodilation are being applied increasingly in the clinical setting in order to detect and monitor the effects of medical therapy and/or lifestyle modifications on coronary circulatory function (8,9,20,78). The use of serial PET myocardial blood flow studies to monitor progression or regression of coronary circulatory (dys)function necessitates establishing the reproducibility of repeated PET MBF measurement (8,97). The re-

producibility of MBF to CPT and measurement error of MBF at rest and during various forms of vasomotor stress along with hemodynamic and biologic factors, that may contribute to the variability in these repeat MBF measurements, are shown in Table 2 (97–102). The reproducibility of hyperemic MBF increases during pharmacologic vasodi-

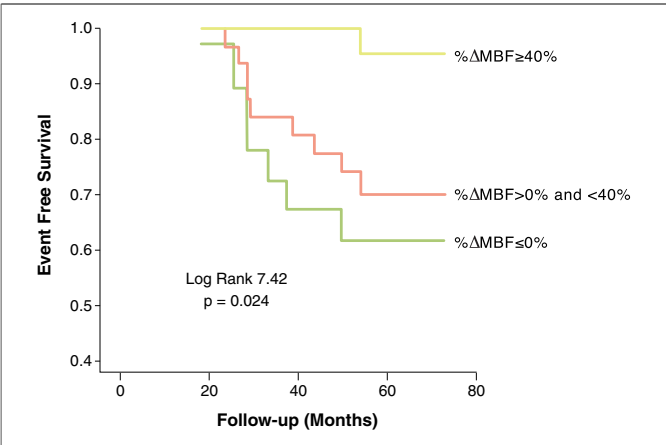


Figure 10. PET-Determined Coronary Endothelial Vasoreactivity and Prognosis
Kaplan-Meier analyses in patients with cardiovascular risk factors and normal coronary angiograms undergoing assessment of myocardial blood flow (MBF) response to cold pressor test (CPT) with positron emission tomography (PET). Attenuation of PET-measured and endothelium-related MBF responses to sympathetic stimulation with cold pressor testing are associated with a higher risk for cardiac events (during long-term follow-up) as compared with those with normal flow increases; normal (%ΔMBF ≥40%), impaired (%ΔMBF >0% and <40%), and decreased (%ΔMBF ≤0%). Reproduced with permission from Schindler et al. (12).

Table 2. MBF and Hemodynamics at Measurements 1 (m = 1) and 2 (m = 2) on the Same Day and Measurement 3 (m = 3) After 2 Weeks for All Study Participants (N = 20)

	m = 1	CV	m = 2	CV	m = 3	CV	Absolute Mean Difference m = 12	Absolute Mean Difference m = 13
MBF in ml/g/min								
At rest	0.67 ± 0.19	0.29	0.66 ± 0.15	0.22	0.63 ± 0.18	0.28	0.09 ± 0.10	0.10 ± 0.10
During CPT	0.88 ± 0.21	0.24	0.85 ± 0.20	0.23	0.82 ± 0.21	0.13	0.11 ± 0.09	0.14 ± 0.10
Δ Change to CPT	0.21 ± 0.17	0.79	0.19 ± 0.16	0.83	0.19 ± 0.14	0.41	0.08 ± 0.05	0.19 ± 0.10
Hemodynamics at rest								
Heart rate (beats/min)	61 ± 7	0.12	62 ± 9	0.13	61 ± 9	0.16	2.5 ± 2.2	7.1 ± 5.0
SBP (mm Hg)	116 ± 12	0.11	120 ± 15	0.12	115 ± 13	0.11	5.5 ± 7.6	6.6 ± 5.6
DBP (mm Hg)	71 ± 7	0.10	73 ± 6	0.08	69 ± 8	0.11	3.0 ± 2.6*	5.5 ± 5.3
RPP (mm Hg/min)	7,113 ± 1,161	0.16	7,349 ± 1,157	0.16	6,936 ± 986	0.14	430 ± 445	789 ± 691
Hemodynamics during CPT								
Heart rate (beats/min)	68 ± 8	0.12	67 ± 7	0.11	67 ± 9	0.14	3.5 ± 2.4	5.8 ± 5.1
SBP (mm Hg)	148 ± 22	0.15	152 ± 22	0.15	149 ± 23	0.16	5.8 ± 10	8.3 ± 11
DBP (mm Hg)	86 ± 11	0.13	87 ± 12	0.14	85 ± 13	0.15	2.7 ± 2.1	8.5 ± 6.9
RPP (mm Hg/min)	9,982 ± 1,798	0.18	10,160 ± 1,456	0.14	9,935 ± 1,259	0.18	724 ± 543	1,470 ± 1,011
ΔRPP (mm Hg/min)	2,869 ± 1,666	0.58	2,811 ± 1,300	0.46	2,999 ± 1,740	0.58	762 ± 517	1,046 ± 857

*p ≤ 0.05 for difference by paired t test; p = NS for intragroup comparisons between coefficients of variation (CV) 1 to 3 by analysis of variance (Levene test). Reproduced with permission from Schindler et al. (97).
CPT = cold pressor testing; DBP = diastolic blood pressure; MBF = myocardial blood flow; RPP = rate–pressure product; SBP = systolic blood pressure.

lation and bicycle exercise using ^{13}N -ammonia, ^{15}O -labeled water or ^{82}Rb with PET are reasonable and in the range of 4 to 15% (99,103–105). Also when CPT-related MBFs were measured with ^{15}O -labeled water on a 1-day protocol, the MBFs appeared to be reproducible within 27% (106). In a more comprehensive investigation (97), the hemodynamic and endothelium-related MBF responses to CPT from rest (ΔMBF), as measured with ^{13}N -ammonia and PET, were demonstrated to be not only highly reproducible in short-term (1-day protocol), but also in long-term (2- to 3-weeks protocol) within a range of 10% (Table 2). In this regard, the range of measurement errors, as indicated by the standard error of the estimate (SEE) from the Pearson correlation coefficient (r) of the least-square regression for the endothelium-related ΔMBF to CPT determined with ^{13}N -ammonia PET, was observed to be 0.09 ml/g/min for short-term and 0.17 ml/g/min for long-term repeat measurements (Table 2). According to these values of SEE, changes in ΔMBF to CPT in serial medical intervention and/or lifestyle modification studies are likely to exceed this range of SEE (97). Applying the mean difference and the corresponding standard deviation (SD) of repeat MBF assessment in Table 2, one can derive the sample size of a study population that would be needed to sufficiently power a serial MBF PET study. For example, using the longitudinal mean difference and the

corresponding SD of the ΔMBF to CPT of 0.08 ± 0.05 ml/g/min in the short-term and of 0.19 ± 0.10 ml/g/min in the long-term, at a 5% significance level with a power of 87%, a sample size of 14 and 22 individuals would be needed for serial ^{13}N -ammonia PET flow studies in order to identify possible intervention-related, statistically significant alterations in MBF responses to CPT (97). Another useful statistical parameter commonly referred to in the interpretation of reproducibility data is the repeatability coefficient as suggested by Bland and Altman (107), which denotes the agreement between repeat measurements. Conversely, the repeatability coefficient can also be used as an index for direct comparison of the precision of MBF measurements between PET flow studies that have utilized different radiotracers (97). For example, the repeatability coefficient for short- and long-term reproducibility measurements of ΔMBF to CPT with ^{13}N -ammonia PET were lower than those for hyperemic MBF increases reported previously (99,104,108).

Monitoring Therapy

According to the Framingham Heart Study (4), individuals with a high cardiovascular risk profile, such as type 2 diabetes mellitus or multiple coronary risk factors, are at risk for future cardiovascular events, and are commonly referred for primary and secondary medical prevention of CAD (5–7). Indi-

viduals with an intermediate cardiovascular risk, however, may not necessarily be considered for preventive medical interventions and/or life style modifications. In this regard, assessment of coronary vascular or circulatory function with PET may further risk stratify these individuals with an intermediate cardiovascular risk (8–10). Other possible surrogate markers for subclinical CAD include measurements in carotid intima-media thickness determined by vascular ultrasound (15), or coronary artery calcification and/or coronary morphology by multidetector CT (16,17). Assessment of functional abnormalities of the coronary vessels with PET may have an advantage over structural alterations of the arterial wall, as it may identify the earliest functional stage of the initiation and development of the coronary atherosclerotic process before structural alterations within the arterial wall may manifest (18). If CAD-related functional abnormalities of the coronary circulation precede morphologic changes of the vessels (8,9,19,20), then PET could emerge as a promising tool to better identify asymptomatic individuals with an intermediate or even low cardiovascular risk, who are likely to benefit from an early initiation or intensified medical preventive therapy (8,21). Further, given the pivotal role of functional abnormalities of the coronary circulation in the development and progression of atherosclerosis, an improvement or even restoration of PET-determined coronary circulatory dysfunction in response to various forms of vasomotor

stress by a variety of preventive medical interventions, such as angiotensin-converting enzyme inhibitors (75), beta-hydroxymethylglutaryl coenzyme A reductase inhibitors (109), hormone replacement therapy in post-menopausal women (48,89), insulin-sensitizing thiazolidinedione in insulin-resistant individuals (88), euglycemic control in diabetes, and physical exercise (110,111), has become a primary therapeutic strategy for prevention of the atherosclerotic process. Notably, some preliminary observations in the assessment of vascular function of the peripheral circulation may strongly suggest that a normalization of endothelium-dependent vascular function by preventive medical intervention may indeed lead to an improved cardiovascular outcome (112,113). Among patients presenting with acute coronary syndrome and treated with standard medical therapy, the group that normalized their endothelial function (assessed at the forearm) was paralleled by an event-free survival, but not in those patients who did not normalize their endothelial function (112). In post-menopausal hypertensive women, an improvement in brachial artery flow-mediated (endothelium-dependent) vasodilation after installation of aggressive antihypertensive therapy resulted in an improved clinical outcome (113). In view of these preliminary findings, PET assessment of MBF responses to vasomotor stress may prove as an unique tool to noninvasively identify and characterize coronary circulatory dysfunction, as func-

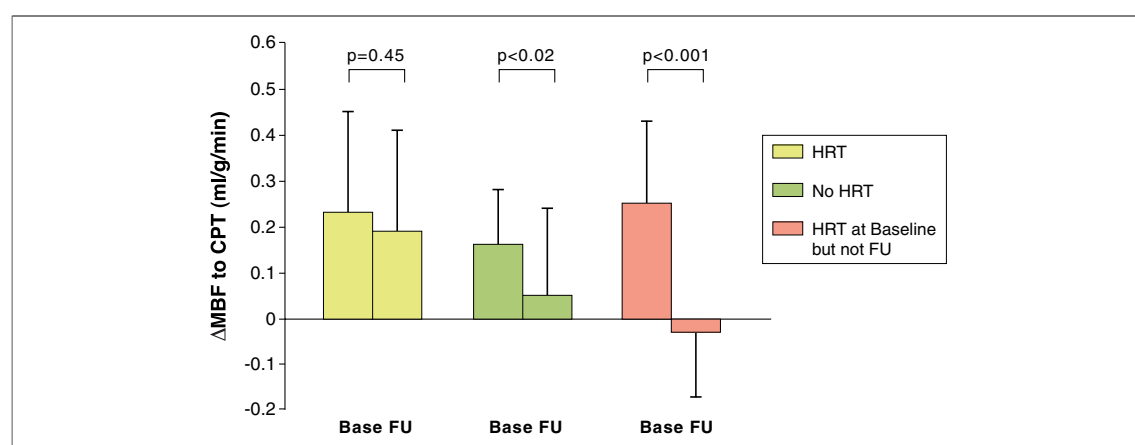


Figure 11. Hormone Replacement and PET-Determined Coronary Endothelial Vasoreactivity in Post-Menopausal Women

Effect of hormone replacement therapy (HRT) on coronary endothelial dysfunction in post-menopausal women with medically treated cardiovascular risk factors. The endothelium-related change in myocardial blood flow (Δ MBF) from rest to cold pressor testing (CPT) at baseline (Base) and follow-up (FU) among different groups are shown. In post-menopausal women with HRT at baseline and follow-up, the Δ MBF response to CPT was generally maintained, whereas in the women without HRT, there was a significant decrease in Δ MBF to CPT. Interestingly, the Δ MBF to CPT in post-menopausal women who had discontinued HRT during follow-up was even worse than in those women who had never been on HRT, suggesting perhaps a “rebound” phenomenon on coronary endothelial (dys)function. Reproduced with permission from Schindler et al. (48). PET = positron emission tomography.

tional precursor of CAD, and to monitor the success of effects of pharmacologic interventions or lifestyle modification on the functioning of the coronary circulation in asymptomatic cardiovascular risk individuals or in patients with clinically manifest CAD (8,114). Using PET measurements of MBF in response to CPT to evaluate coronary endothelial function, a divergent response after medical control of blood pressures with the angiotensin II receptor blocker olmesartan and with the calcium antagonist amlodipine was observed (116). Whereas angiotensin II receptor blocker improved coronary endothelial function, no such beneficial effect was observed for the calcium antagonist amlodipine. Most likely, specific antioxidative effects of angiotensin II receptor blocker accounted for the improvement in coronary endothelial function and, thereby, mediated vascular resistance against the development of CAD in these hypertensive patients. PET flow studies also contributed to unmask beneficial effects of hormone replacement therapy with medically treated cardiovascular risk factors (48). As it was observed, hormone replacement therapy with estrogen alone or in concert with a progesterone in post-menopausal women, in addition to standard preventive medical intervention of traditional cardiovascular risk factors, contributed to preserve the functional integrity of the coronary endothelium (Fig. 11). Conceptually, a normal function of the coronary circulation in cardiovascular risk individuals in fact should exert numerous vasoprotective effects against the development of CAD-related structural disease, predominantly mediated through the release of atheroprotective and endothelium-derived nitric oxide (8). If this holds true, then a normalization of coronary circulatory function in cardiovascular risk individuals should prevent the manifestation and/or progression of a CAD process. Indeed, as recent investigations suggest (115), an improvement of endothelium-related MBF responses to CPT in type 2 diabetes

mellitus after 1-year follow-up in response to glucose lowering treatment with metformin and/or glyburide may mediate direct preventive effects on the progression of epicardial structural disease. Although these preliminary observations of PET flow studies strongly support the evolving concept that improvement in coronary circulatory function in asymptomatic cardiovascular risk individuals or in patients with clinically manifest CAD may lead to an improved clinical outcome, it remains to be tested in further prospective, large-scale clinical trials.

Conclusions

Assessment of stress-induced myocardial perfusion defects have been firmly established as an important diagnostic and prognostic tool for the evaluation of patients with suspected CAD. Cardiac PET in conjunction with tracer-kinetic modeling for ^{13}N -ammonia, ^{15}O -water, or ^{82}Rb affords the assessment of regional MBF of the left ventricle in absolute units in ml/g/min, which adds a new dimension to the noninvasive evaluation of the CAD process. By assessing MBFs and the MFR noninvasively, PET may identify early functional and/or structural abnormalities of the coronary artery circulation before its progression to symptomatic CAD ensues. In particular, the identification and characterization of the vasodilator capacity and endothelial reactivity of the coronary circulation may guide decisions for medical therapy as well as monitor the effects of pharmacologic interventions, risk factor modification, or lifestyle changes. The aim of image-guided and personalized preventive vascular medicine may soon be attainable with PET technology.

Reprint requests and correspondence: Dr. Thomas H. Schindler, Department of Internal Medicine, Cardiovascular Center, 6th Floor, Nuclear Cardiology, University Hospitals of Geneva, Rue Gabrielle-Perret-Gentil 4, CH-1211 Geneva, Switzerland. E-mail: thomas.schindler@hcuge.ch.

REFERENCES

- Vedanthan R, Fuster V. Disease prevention: the moving target of global cardiovascular health. *Nat Rev Cardiol* 2009;6:327–8.
- Eckel RH, Daniels SR, Jacobs AK, Robertson RM. America's children: a critical time for prevention. *Circulation* 2005;111:1866–8.
- Mendelsohn ME, Karas RH. HRT and the young at heart. *N Engl J Med* 2007;356:2639–41.
- Wilson PW, D'Agostino RB, Levy D, Belanger AM, Silbershatz H, Kannel WB. Prediction of coronary heart disease using risk factor categories. *Circulation* 1998;97:1837–47.
- Yusuf S, Sleight P, Pogue J, Bosch J, Davies R, Dagenais G. Effects of an angiotensin-converting-enzyme inhibitor, ramipril, on cardiovascular events in high-risk patients. The Heart Outcomes Prevention Evaluation Study Investigators. *N Engl J Med* 2000;342:145–53.
- Randomised trial of cholesterol lowering in 4444 patients with coronary heart disease: the Scandinavian Simvastatin Survival Study (4S). *Lancet* 1994;344:1383–9.
- Dormandy JA, Charbonnel B, Eckland DJ, et al. Secondary prevention of macrovascular events in patients with type 2 diabetes in the PROactive Study (PROspective pioglitAzone Clinical Trial In macroVascular Events): a randomised controlled trial. *Lancet* 2005; 366:1279–89.

8. Schindler TH, Zhang XL, Vincenti G, Mhiri L, Lerch R, Schelbert HR. Role of PET in the evaluation and understanding of coronary physiology. *J Nucl Cardiol* 2007;14:589–603.
9. Camici PG, Crea F. Coronary microvascular dysfunction. *N Engl J Med* 2007;356:830–40.
10. Neglia D, Michelassi C, Trivieri MG, et al. Prognostic role of myocardial blood flow impairment in idiopathic left ventricular dysfunction. *Circulation* 2002;105:186–93.
11. Lerman A, Zeiher AM. Endothelial function: cardiac events. *Circulation* 2005;111:363–8.
12. Schindler TH, Nitzsche EU, Schelbert HR, et al. Positron emission tomography-measured abnormal responses of myocardial blood flow to sympathetic stimulation are associated with the risk of developing cardiovascular events. *J Am Coll Cardiol* 2005;45:1505–12.
13. Herzog BA, Husmann L, Valenta I, et al. Long-term prognostic value of ¹³N-ammonia myocardial perfusion positron emission tomography added value of coronary flow reserve. *J Am Coll Cardiol* 2009;54:150–6.
14. Tio RA, Dabeshlim A, Siebelink HM, et al. Comparison between the prognostic value of left ventricular function and myocardial perfusion reserve in patients with ischemic heart disease. *J Nucl Med* 2009;50:214–9.
15. Graner M, Varpula M, Kahri J, et al. Association of carotid intima-media thickness with angiographic severity and extent of coronary artery disease. *Am J Cardiol* 2006;97:624–9.
16. Hoffmann U, Nagurney JT, Moselewski F, et al. Coronary multidetector computed tomography in the assessment of patients with acute chest pain. *Circulation* 2006;114:2251–60.
17. Achenbach S, Dilsizian V, Kramer CM, Zoghbi WA. The year in coronary artery disease. *J Am Coll Cardiol* 2009;2:774–86.
18. Reddy KG, Nair RN, Sheehan HM, Hodgson JM. Evidence that selective endothelial dysfunction may occur in the absence of angiographic or ultrasound atherosclerosis in patients with risk factors for atherosclerosis. *J Am Coll Cardiol* 1994;23:833–43.
19. Bengel FM, Higuchi T, Javadi MS, Lautamaki R. Cardiac positron emission tomography. *J Am Coll Cardiol* 2009;54:1–15.
20. Camici PG, Rimoldi OE. The clinical value of myocardial blood flow measurement. *J Nucl Med* 2009;50:1076–87.
21. Ganz P, Vita JA. Testing endothelial vasomotor function: nitric oxide, a multipotent molecule. *Circulation* 2003;108:2049–53.
22. Yoshinaga K, Klein R, Tamaki N. Generator-produced rubidium-82 positron emission tomography myocardial perfusion imaging—From basic aspects to clinical applications. *J Cardiol* 2010;55:163–73.
23. Adachi I, Gaemperli O, Valenta I, et al. Assessment of myocardial perfusion by dynamic O-15-labeled water PET imaging: validation of a new fast factor analysis. *J Nucl Cardiol* 2007;14:698–705.
24. Gambhir SS, Schwaiger M, Huang SC, et al. Simple noninvasive quantification method for measuring myocardial glucose utilization in humans employing positron emission tomography and fluorine-18 deoxyglucose. *J Nucl Med* 1989;30:359–66.
25. Weinberg IN, Huang SC, Hoffman EJ, et al. Validation of PET-acquired input functions for cardiac studies. *J Nucl Med* 1988;29:241–7.
26. Schelbert HR. Positron emission tomography of the heart: methodology, findings in the normal and the diseased heart, and clinical applications. In: Phelps M, editor. *PET: Molecular Imaging and Its Biological Applications*. New York, NY: Springer-Verlag 2005;389–508.
27. Vesely MR, Dilsizian V. Nuclear cardiac stress testing in the era of molecular medicine. *J Nucl Med* 2008;49:399–413.
28. Muzik O, Beanlands RS, Hutchins GD, Mangner TJ, Nguyen N, Schwaiger M. Validation of nitrogen-13-ammonia tracer kinetic model for quantification of myocardial blood flow using PET. *J Nucl Med* 1993;34:83–91.
29. Kuhle WG, Porenta G, Huang SC, et al. Quantification of regional myocardial blood flow using ¹³N-ammonia and reoriented dynamic positron emission tomographic imaging. *Circulation* 1992;86:1004–17.
30. Bergmann SR, Fox KA, Rand AL, et al. Quantification of regional myocardial blood flow in vivo with H²¹⁵O. *Circulation* 1984;70:724–33.
31. Araujo LI, Lammertsma AA, Rhodes CG, et al. Noninvasive quantification of regional myocardial blood flow in coronary artery disease with oxygen-15-labeled carbon dioxide inhalation and positron emission tomography. *Circulation* 1991;83:875–85.
32. Schwaiger M, Muzik O. Assessment of myocardial perfusion by positron emission tomography. *Am J Cardiol* 1991;67:35D–43D.
33. Nitzsche EU, Choi Y, Czernin J, Hoh CK, Huang SC, Schelbert HR. Noninvasive quantification of myocardial blood flow in humans. A direct comparison of the [¹³N]ammonia and the [¹⁵O]water techniques. *Circulation* 1996;93:2000–6.
34. Bol A, Melin JA, Vanoverschelde JL, et al. Direct comparison of [¹³N]ammonia and [¹⁵O]water estimates of perfusion with quantification of regional myocardial blood flow by microspheres. *Circulation* 1993;87:512–25.
35. Chow BJ, Beanlands RS, Lee A, et al. Treadmill exercise produces larger perfusion defects than dipyridamole stress N-13 ammonia positron emission tomography. *J Am Coll Cardiol* 2006;47:411–6.
36. Knuuti J, Kajander S, Maki M, Ukonen H. Quantification of myocardial blood flow will reform the detection of CAD. *J Nucl Cardiol* 2009;16:497–506.
37. Machac J, Bacharach SL, Bateman TM, et al. Positron emission tomography myocardial perfusion and glucose metabolism imaging. *J Nucl Cardiol* 2006;13:e121–51.
38. Dilsizian V, Bacharach SL, Beanlands RS, et al. PET myocardial perfusion and metabolism clinical imaging. *J Nucl Cardiol* 2009;16:651.
39. El Fakhri G, Sitek A, Guerin B, Kijewski MF, Di Carli MF, Moore SC. Quantitative dynamic cardiac ⁸²Rb PET using generalized factor and compartment analyses. *J Nucl Med* 2005;46:1264–71.
40. Lin JW, Sciacca RR, Chou RL, Laine AF, Bergmann SR. Quantification of myocardial perfusion in human subjects using ⁸²Rb and wavelet-based noise reduction. *J Nucl Med* 2001;42:201–8.
41. Lortie M, Beanlands RS, Yoshinaga K, Klein R, Dasilva JN, DeKemp RA. Quantification of myocardial blood flow with ⁸²Rb dynamic PET imaging. *Eur J Nucl Med Mol Imaging* 2007;34:1765–74.
42. Nekolla SG, Reder S, Saraste A, et al. Evaluation of the novel myocardial perfusion positron-emission tomography tracer ¹⁸F-BMS-747158-02: comparison to ¹³N-ammonia and validation with microspheres in a pig model. *Circulation* 2009;119:2333–42.
43. Sherif HM, Saraste A, Weidl E, et al. Evaluation of a novel (¹⁸F)-labeled positron-emission tomography perfusion tracer for the assessment of myocardial infarct size in rats. *Circ Cardiovasc Imaging* 2009;2:77–84.

44. Hachamovitch R, Hayes SW, Friedman JD, Cohen I, Berman DS. Stress myocardial perfusion single-photon emission computed tomography is clinically effective and cost effective in risk stratification of patients with a high likelihood of coronary artery disease (CAD) but no known CAD. *J Am Coll Cardiol* 2004;43:200-8.
45. Shaw LJ, Berman DS, Maron DJ, et al. Optimal medical therapy with or without percutaneous coronary intervention to reduce ischemic burden: results from the Clinical Outcomes Utilizing Revascularization and Aggressive Drug Evaluation (COURAGE) trial nuclear substudy. *Circulation* 2008;117:1283-91.
46. Shaw LJ, Min JK, Hachamovitch R, et al. Cardiovascular imaging research at the crossroads. *J Am Coll Cardiol Img* 2010;3:316-24.
47. Hachamovitch R, Kang X, Amanullah AM, et al. Prognostic implications of myocardial perfusion single-photon emission computed tomography in the elderly. *Circulation* 2009;120:2197-206.
48. Schindler TH, Campisi R, Dorsey D, et al. Effect of hormone replacement therapy on vasomotor function of the coronary microcirculation in post-menopausal women with medically treated cardiovascular risk factors. *Eur Heart J* 2009;30:978-86.
49. Schindler TH, Cardenas J, Prior JO, et al. Relationship between increasing body weight, insulin resistance, inflammation, adipocytokine leptin, and coronary circulatory function. *J Am Coll Cardiol* 2006;47:1188-95.
50. Schindler TH, Facta AD, Prior JO, et al. Structural alterations of the coronary arterial wall are associated with myocardial flow heterogeneity in type 2 diabetes mellitus. *Eur J Nucl Med Mol Imaging* 2009;36:219-29.
51. Lima RS, Watson DD, Goode AR, et al. Incremental value of combined perfusion and function over perfusion alone by gated SPECT myocardial perfusion imaging for detection of severe three-vessel coronary artery disease. *J Am Coll Cardiol* 2003;42:64-70.
52. Beller GA. Underestimation of coronary artery disease with SPECT perfusion imaging. *J Nucl Cardiol* 2008;15:151-3.
53. Schindler TH, Valenta I, Dilsizian V. PET assessment of myocardial perfusion. In: Dilsizian V, Pohost GM, editors. *Cardiac CT, PET and MRI*. 2nd edition. Oxford, United Kingdom: Wiley-Blackwell, 2010:95-117.
54. Heller LJ, Cates C, Popma J, et al. Intracoronary Doppler assessment of moderate coronary artery disease: comparison with 201Tl imaging and coronary angiography. FACTS Study Group. *Circulation* 1997;96:484-90.
55. Uren NG, Marraccini P, Gistri R, de Silva R, Camici PG. Altered coronary vasodilator reserve and metabolism in myocardium subtended by normal arteries in patients with coronary artery disease. *J Am Coll Cardiol* 1993;22:650-8.
56. Gould KL. Does coronary flow trump coronary anatomy? *J Am Coll Cardiol Img* 2009;2:1009-23.
57. Gould KL. Coronary flow reserve and pharmacologic stress perfusion imaging: beginnings and evolution. *J Am Coll Cardiol Img* 2009;2:664-9.
58. Berman DS, Kang X, Slomka PJ, et al. Underestimation of extent of ischemia by gated SPECT myocardial perfusion imaging in patients with left main coronary artery disease. *J Nucl Cardiol* 2007;14:521-8.
59. Smith WH, Kastner RJ, Calnon DA, Segalla D, Beller GA, Watson DD. Quantitative gated single photon emission computed tomography imaging: a counts-based method for display and measurement of regional and global ventricular systolic function. *J Nucl Cardiol* 1997;4:451-63.
60. Dorbala S, Hachamovitch R, Curillova Z, et al. Incremental prognostic value of gated Rb-82 positron emission tomography myocardial perfusion imaging over clinical variables and rest LVEF. *J Am Coll Cardiol Img* 2009;2:846-54.
61. Dorbala S, Vangala D, Sampson U, Limaye A, Kwong R, Di Carli MF. Value of vasodilator left ventricular ejection fraction reserve in evaluating the magnitude of myocardium at risk and the extent of angiographic coronary artery disease: a 82Rb PET/CT study. *J Nucl Med* 2007;48:349-58.
62. Pichler BJ, Wehrl HF, Judenhofer MS. Latest advances in molecular imaging instrumentation. *J Nucl Med* 2008;49 Suppl 2:5S-23S.
63. Sampson UK, Dorbala S, Limaye A, Kwong R, Di Carli MF. Diagnostic accuracy of rubidium-82 myocardial perfusion imaging with hybrid positron emission tomography/computed tomography in the detection of coronary artery disease. *J Am Coll Cardiol* 2007;49:1052-8.
64. Di Carli MF. Advances in positron emission tomography. *J Nucl Cardiol* 2004;11:719-32.
65. Bateman TM, Heller GV, McGhie AJ, et al. Diagnostic accuracy of rest/stress ECG-gated Rb-82 myocardial perfusion PET: comparison with ECG-gated Tc-99m sestamibi SPECT. *J Nucl Cardiol* 2006;13:24-33.
66. Go RT, Marwick TH, MacIntyre WJ, et al. A prospective comparison of rubidium-82 PET and thallium-201 SPECT myocardial perfusion imaging utilizing a single dipyridamole stress in the diagnosis of coronary artery disease. *J Nucl Med* 1990;31:1899-905.
67. Stewart RE, Schwaiger M, Molina E, et al. Comparison of rubidium-82 positron emission tomography and thallium-201 SPECT imaging for detection of coronary artery disease. *Am J Cardiol* 1991;67:1303-10.
68. Keane D, Haase J, Slager CJ, et al. Comparative validation of quantitative coronary angiography systems. Results and implications from a multicenter study using a standardized approach. *Circulation* 1995;91:2174-83.
69. Uren NG, Melin JA, De Bruyne B, Wijns W, Baudhuin T, Camici PG. Relation between myocardial blood flow and the severity of coronary-artery stenosis. *N Engl J Med* 1994;330:1782-8.
70. Krivokapich J, Czernin J, Schelbert HR. Dobutamine positron emission tomography: absolute quantitation of rest and dobutamine myocardial blood flow and correlation with cardiac work and percent diameter stenosis in patients with and without coronary artery disease. *J Am Coll Cardiol* 1996;28:565-72.
71. Di Carli M, Czernin J, Hoh CK, et al. Relation among stenosis severity, myocardial blood flow, and flow reserve in patients with coronary artery disease. *Circulation* 1995;91:1944-51.
72. Demer LL, Gould KL, Goldstein RA, et al. Assessment of coronary artery disease severity by positron emission tomography. Comparison with quantitative arteriography in 193 patients. *Circulation* 1989;79:825-35.
73. Sato A, Hiroe M, Tamura M, et al. Quantitative measures of coronary stenosis severity by 64-slice CT angiography and relation to physiologic significance of perfusion in nonobese patients: comparison with stress myocardial perfusion imaging. *J Nucl Med* 2008;49:564-72.
74. Baller D, Notohamiprodjo G, Gleichmann U, Holzinger J, Weise R, Lehmann J. Improvement in coronary flow reserve determined by positron emission tomography after 6 months of cholesterol-lowering therapy in patients with early stages of coronary atherosclerosis. *Circulation* 1999;99:2871-5.

75. Mancini GB, Henry GC, Macaya C, et al. Angiotensin-converting enzyme inhibition with quinapril improves endothelial vasomotor dysfunction in patients with coronary artery disease. The TREND (Trial on Reversing ENdothelial Dysfunction) Study. *Circulation* 1996;94:258-65.
76. Meier P, Gloekler S, Zbinden R, et al. Beneficial effect of recruitable collaterals: a 10-year follow-up study in patients with stable coronary artery disease undergoing quantitative collateral measurements. *Circulation* 2007;116:975-83.
77. Hajjiri MM, Leavitt MB, Zheng H, Spooner AE, Fischman AJ, Gewirtz H. Comparison of positron emission tomography measurement of adenosine-stimulated absolute myocardial blood flow versus relative myocardial tracer content for physiological assessment of coronary artery stenosis severity and location. *J Am Coll Cardiol* 2009;2:751-8.
78. Camici PG. Absolute figures are better than percentages. *J Am Coll Cardiol* 2009;2:759-60.
79. Nesterov SV, Han C, Maki M, et al. Myocardial perfusion quantitation with (15)O-labelled water PET: high reproducibility of the new cardiac analysis software (Carimas). *Eur J Nucl Med Mol Imaging* 2009;36:1594-602.
80. Anagnostopoulos C, Almonacid A, El Fakhri G, et al. Quantitative relationship between coronary vasodilator reserve assessed by 82Rb PET imaging and coronary artery stenosis severity. *Eur J Nucl Med Mol Imaging* 2008;35:1593-601.
81. Prior JO, Quinones MJ, Hernandez-Pampaloni M, et al. Coronary circulatory dysfunction in insulin resistance, impaired glucose tolerance, and type 2 diabetes mellitus. *Circulation* 2005;111:2291-8.
82. Kaufmann PA, Gnechi-Ruscone T, Schafers KP, Luscher TF, Camici PG. Low density lipoprotein cholesterol and coronary microvascular dysfunction in hypercholesterolemia. *J Am Coll Cardiol* 2000;36:103-9.
83. Melikian N, De Bondt P, Tonino P, et al. Fractional flow reserve and myocardial perfusion imaging in patients with angiographic multivessel coronary artery disease. *J Am Coll Cardiol* 2003;41:307-14.
84. Beller GA, Ragosta M. Decision making in multivessel coronary disease: the need for physiological lesion assessment. *J Am Coll Cardiol* 2003;41:315-7.
85. Tsukamoto T, Morita K, Naya M, et al. Myocardial flow reserve is influenced by both coronary artery stenosis severity and coronary risk factors in patients with suspected coronary artery disease. *Eur J Nucl Med Mol Imaging* 2006;33:1150-6.
86. Dorbala S, Hassan A, Heinonen T, Schelbert HR, Di Carli MF. Coronary vasodilator reserve and Framingham risk scores in subjects at risk for coronary artery disease. *J Nucl Cardiol* 2006;13:761-7.
87. Britten MB, Zeiher AM, Schachinger V. Microvascular dysfunction in angiographically normal or mildly diseased coronary arteries predicts adverse cardiovascular long-term outcome. *Coron Artery Dis* 2004;15:259-64.
88. Quinones MJ, Hernandez-Pampaloni M, Schelbert H, et al. Coronary vasomotor abnormalities in insulin-resistant individuals. *Ann Intern Med* 2004;140:700-8.
89. Campisi R, Nathan L, Pampaloni MH, et al. Noninvasive assessment of coronary microcirculatory function in postmenopausal women and effects of short-term and long-term estrogen administration. *Circulation* 2002;105:425-30.
90. Campisi R, Czernin J, Schoder H, Sayre JW, Schelbert HR. L-Arginine normalizes coronary vasomotion in long-term smokers. *Circulation* 1999;99:491-7.
91. Schindler TH, Nitzsche EU, Olshewski M, et al. Chronic inflammation and impaired coronary vasoreactivity in patients with coronary risk factors. *Circulation* 2004;110:1069-75.
92. Munzel T, Daiber A, Ullrich V, Mulsch A. Vascular consequences of endothelial nitric oxide synthase uncoupling for the activity and expression of the soluble guanylyl cyclase and the cGMP-dependent protein kinase. *Arterioscler Thromb Vasc Biol* 2005;25:1551-7.
93. Marwick TH, Shan K, Patel S, Go RT, Lauer MS. Incremental value of rubidium-82 positron emission tomography for prognostic assessment of known or suspected coronary artery disease. *Am J Cardiol* 1997;80:865-70.
94. Yoshinaga K, Chow BJ, Williams K, et al. What is the prognostic value of myocardial perfusion imaging using rubidium-82 positron emission tomography? *J Am Coll Cardiol* 2006;48:1029-39.
95. Cecchi F, Olivetto I, Gistri R, Lorenzoni R, Chiriaci G, Camici PG. Coronary microvascular dysfunction and prognosis in hypertrophic cardiomyopathy. *N Engl J Med* 2003;349:1027-35.
96. Bonetti PO, Lerman LO, Lerman A. Endothelial dysfunction: a marker of atherosclerotic risk. *Arterioscler Thromb Vasc Biol* 2003;23:168-75.
97. Schindler TH, Zhang XL, Prior JO, et al. Assessment of intra- and inter-observer reproducibility of rest and cold pressor test-stimulated myocardial blood flow with (13)N-ammonia and PET. *Eur J Nucl Med Mol Imaging* 2007;34:1178-88.
98. Sawada S, Muzik O, Beanlands RS, Wolfe E, Hutchins GD, Schwaiger M. Interobserver and interstudy variability of myocardial blood flow and flow-reserve measurements with nitrogen 13 ammonia-labeled positron emission tomography. *J Nucl Cardiol* 1995;2:413-22.
99. Kaufmann PA, Gnechi-Ruscone T, Yap JT, Rimoldi O, Camici PG. Assessment of the reproducibility of baseline and hyperemic myocardial blood flow measurements with 15O-labeled water and PET. *J Nucl Med* 1999;40:1848-56.
100. Schindler TH, Nitzsche EU, Olshewski M, et al. PET-measured responses of MBF to cold pressor testing correlate with indices of coronary vasomotion on quantitative coronary angiography. *J Nucl Med* 2004;45:419-28.
101. Czernin J, Muller P, Chan S, et al. Influence of age and hemodynamics on myocardial blood flow and flow reserve. *Circulation* 1993;88:62-9.
102. Manabe O, Yoshinaga K, Katoh C, Naya M, deKemp RA, Tamaki N. Repeatability of rest and hyperemic myocardial blood flow measurements with 82Rb dynamic PET. *J Nucl Med* 2009;50:68-71.
103. Nagamachi S, Czernin J, Kim AS, et al. Reproducibility of measurements of regional resting and hyperemic myocardial blood flow assessed with PET. *J Nucl Med* 1996;37:1626-31.
104. Wyss CA, Koepfli P, Mikolajczyk K, Burger C, von Schulthess GK, Kaufmann PA. Bicycle exercise stress in PET for assessment of coronary flow reserve: repeatability and comparison with adenosine stress. *J Nucl Med* 2003;44:146-54.
105. El Fakhri G, Kardan A, Sitek A, et al. Reproducibility and accuracy of quantitative myocardial blood flow assessment with 82Rb PET: comparison with 13N-ammonia PET. *J Nucl Med* 2009;50:1062-71.
106. Siegrist PT, Gaemperli O, Koepfli P, et al. Repeatability of cold pressor test-induced flow increase assessed with H(2)(15)O and PET. *J Nucl Med* 2006;47:1420-6.

107. Bland JM, Altman DG. Statistical methods for assessing agreement between two methods of clinical measurement. *Lancet* 1986;1:307-10.
108. Jagathesan R, Kaufmann PA, Rosen SD, et al. Assessment of the long-term reproducibility of baseline and dobutamine-induced myocardial blood flow in patients with stable coronary artery disease. *J Nucl Med* 2005;46:212-9.
109. Wielepp P, Baller D, Gleichmann U, Pulawski E, Horstkotte D, Burchert W. Beneficial effects of atorvastatin on myocardial regions with initially low vasodilatory capacity at various stages of coronary artery disease. *Eur J Nucl Med Mol Imaging* 2005;32:1371-7.
110. Schindler TH, Facta AD, Prior JO, et al. Improvement in coronary vascular dysfunction produced with euglycaemic control in patients with type 2 diabetes. *Heart* 2007;93:345-9.
111. Czernin J, Barnard RJ, Sun KT, et al. Effect of short-term cardiovascular conditioning and low-fat diet on myocardial blood flow and flow reserve. *Circulation* 1995;92:197-204.
112. Fichtlscherer S, Breuer S, Zeiher AM. Prognostic value of systemic endothelial dysfunction in patients with acute coronary syndromes: further evidence for the existence of the "vulnerable" patient. *Circulation* 2004;110:1926-32.
113. Modena MG, Bonetti L, Coppi F, Bursi F, Rossi R. Prognostic role of reversible endothelial dysfunction in hypertensive postmenopausal women. *J Am Coll Cardiol* 2002;40:505-10.
114. Schelbert HR. Quantifying myocardial perfusion for the assessment of preclinical CAD. In: Di Carli MF and Lipton MJ, editors. *Cardiac PET and PET/CT Imaging*. New York, NY: Springer, 2007:166-77.
115. Schindler TH, Cadenas J, Facta AD, et al. Improvement in coronary endothelial function is independently associated with a slowed progression of coronary artery calcification in type 2 diabetes mellitus. *Eur Heart J* 2009;30:3064-73.
116. Naya M, Tsukamoto T, Morita K, et al. Olmesartan but not amlodipine, improves endothelium-dependent coronary dilation in hypertensive patients. *J Am Coll Cardiol* 2007;50:1144-9.

Key Words: cardiovascular disease prevention ■ coronary artery disease ■ coronary circulation ■ endothelium ■ microcirculation ■ myocardial blood flow ■ myocardial flow reserve ■ positron emission tomography.